Published December 11, 2015

Determining Evapotranspiration of a Chinese Willow Stand with Three-Needle Heat-Pulse Probes

Sheng Wang
Jun Fan*
Quanjiu Wang
State Key Lab. of Soil Erosion and Dryland Farming on the Loess Plateau
Institute of Soil and Water Conservation
Chinese Academy of Sciences and Ministry of Water Resources
Xinong Road 26
Yangling
Shaanxi Province 712100
P. R. China

Quantifying evapotranspiration (ET) and partitioning it into its individual components, evaporation (E) and transpiration (T), is essential to understanding eco-hydrological systems and guiding agricultural production practices. Our study tested the possibility of using heat-pulse probes (HPP) to determine E, T, and ET. Values of E and T were determined using the sensible heat balance theory and heat ratio method (HRM), respectively. Field experiments were conducted in a small stand of 10 *Salix matsudana* trees growing in a sandy soil on the Loess Plateau, China. An arrangement of five three-needle HPP sets determined E throughout the 3- to 33-mm soil layer. Sap flux density (v_s) was determined by three HPP-sets inserted in the sapwood of three sample trees at breast height; up-scaling was used to determine T at the stand level. Summing E and T gave the stand ET. The HPP E, v_s, and ET values were compared with those obtained from microlysimeters (MLS), thermal diffusion probes (TDP), and the water budget method, respectively. Daily HPP E had a moderate, but significant (R^2 = 0.47; P < 0.001) linear relationship with MLS E. Total HPP E was 13.4% lower than MLS E. Hourly HPP v_s had a highly significant linear relationship (R^2 = 0.87; P < 0.001) to TDP v_s but was consistently underestimated by 49%. Adjusting the original wound-size correction factor removed this bias. Summing the HPP E (67.3 mm) and T (89.0 mm) gave the ET (156.3 mm), which was 21.0 mm higher than the water budget ET estimate. We concluded that using HPP to estimate ET, E, and T was a promising approach, suitable for providing long-term, continuous, in situ, and high time-resolution estimations, even though certain issues still need to be resolved.

Abbreviations: ABC, adiabatic boundary condition; DBH, diameter at breast height; DOY, day of year; E, evaporation; ET, evapotranspiration; HPP, heat-pulse probe; HRM, heat ratio method; MBE, mean bias error; MLS, microlysimeter; PILS, pulsed infinite line source; RMSE, root-mean-square error; SHB, sensible heat balance; T, transpiration; TDP, thermal diffusion probe; v_s, sap flux density; VWC, volumetric water content.

Evapotranspiration is an important variable that needs to be determined to understand eco-hydrological systems and that represents a significant proportion of the water balance in those systems, especially in arid regions (Kool et al., 2014). Globally ET consumes almost 25% of the solar energy input (Trenberth et al., 2009). Within the global hydrological cycle ET returns about 60% of the terrestrial precipitation to the atmosphere (Oki and Kanae, 2006). As an energy-intensive hydrographic process, ET affects the costs of agriculture, engineering, and industry (Or et al., 2013). Quantifying ET is of critical importance when assessing changes in hydrologic reservoirs and surface energy balances, and for many practical applications. The individual components of ET include the E of water from porous soils and its T through the stomata of plants. The function of E and T within ecosystems is distinctly different: T is usually associated with plant productivity, whereas E does not directly contribute to plant production. The partitioning of ET into its E and T components gives a better understanding of water-use efficiency, or water productivity, where T is commonly considered the

Soil Sci. Soc. Am. J. 79:1545–1555
doi:10.2136/sssaj2015.05.0180
Received 7 May 2015
Accepted 10 Aug. 2015.
*Corresponding author: (fanjun@ms.iswc.ac.cn).

desirable component while E is undesirable (Agam et al., 2012; van Halsema and Vincent, 2012). In agriculture, an accurate estimation of ET and its partitioning is essential when determining water management practices, designing irrigation systems and irrigation regimes, and calculating potential crop yields. For example, it is estimated that 80% of the freshwater in Asia is used for irrigation, and a better understanding of the partitioning of the ET components could help determine if irrigation could be improved and available water could be used more productively (Zhao et al., 2013).

Numerous measuring and modeling methods can be applied to quantify ET. Evapotranspiration can be measured by a range of methods, such as, the water budget, surface energy budget, mass balance, and eddy correlation approaches, etc. Evapotranspiration can also be quantified by modeling, such as, the well-known approach of using the FAO Penman–Monteith equations to obtain the reference ET, and crop coefficients to obtain the ET for a specific crop (Allen, 2000). Kool et al. (2014) reviewed thoroughly the available means by which to partition ET. However, E and T components are rarely measured separately and simultaneously in practice despite the importance of partitioning ET into E and T being widely acknowledged.

The HPP was first used to determine soil thermal properties, including soil heat capacity, soil thermal diffusivity, and thermal conductivity (Campbell et al., 1991; Bristow et al., 1994; Zhang et al., 2014). Subsequently, HPP was used to measure soil water content, which could be related directly to heat capacity (Ochsner et al., 2003), soil water flux (Ochsner et al., 2005), soil heat shortage (Ochsner et al., 2007), and soil bulk density (Liu et al., 2008). Heitman et al. (2008a; 2008b) investigated subsurface soil E dynamics revealed by sensible heat observations obtained using a three-needle HPP arrangement. A major advantage of HPP was that such observations could be made in situ and continuously. This advantage has led to numerous studies that have assessed and utilized HPP to measure evaporation using either the three-needle HPP combination (Sakai et al., 2011; Trautz et al., 2014) or a modified 11-needle HPP arrangement (Xiao et al., 2012, 2014).

Sap flow can be determined using thermal-based techniques that obtain water flow through the stem following various methodologies (Cermak et al., 2004; Vandegehuchte and Steppe, 2013). It is estimated that up to 95% of the water absorbed by roots is lost via T through plant leaves. Thus, an approximation of tree T can be accurately estimated from the stem sap flow. Methods can mainly be categorized into the heat balance, heat-pulse, and constant heater methods. The HRM was developed by Burgess et al. (2001) using heat-pulse observations. It uses the ratio of temperature increases, which occur for a short period following the emission of a heat pulse at equally distanced downstream and upstream locations, to determine the sap flow. It is especially effective for low and even reverse flow determinations for woody plants. The probe used in the HRM consists of two temperature sensor needles at equal distances from a central needle that acts as the source of the emitted heat pulse; this construction primarily differs from HPP used for subsurface soil evaporation determinations in that it lacks a temperature sensor in the central needle. Due to this similarity, it follows that the HPP, widely applied in subsurface soil E determinations, can potentially be used in determining sap flow. The sap flow can then be used to obtain tree stand T after up-scaling from the tree to the stand level.

To the best of our knowledge, there are no reports of E and T determinations that are both made with HPP before being combined to obtain ET. In northwest China, many relatively small, monoculture vegetation areas exist, for example, as tree stands or areas of shrub land (Yu and Sun, 2013). Over the past three decades, the number of such areas have increased and the ecosystem health has been greatly improved in response to vegetation restoration projects, such as the "Three north shelterbelt program" and the "Grain-for-Green project" (Qi et al., 2011). Such restoration projects often encounter problems connected to the water use of the new land use types (Jiang et al., 2015). Knowledge of ET and its components is essential to address these issues, and using HPP would be a potential approach to quantifying ET and its components. The objective of this study was to test the possibility of estimating ET as a combination of E and T determinations made using the same three-needle HPP-type in a small stand of Chinese willow (*Salix matsudana*) on the Loess Plateau. Comparisons of these results were then made with alternative determinations of E, v_s (which could be then transformed to T) and ET using MLS, TDP, and the water budget method, respectively, to evaluate the HPP approach.

MATERIALS AND METHODS

Site Description

The study was performed in a small sparse stand of 10 *S. matsudana* Koidz trees in the Liudaogou catchment (1200 m altitude, 38.78°N, 110.35°E) of Shenmu County, Shaanxi Province, China. The catchment is in a part of the Loess Plateau referred to as the "water-wind erosion crisscross region", where severe soil losses occur due to a combination of water and wind erosion processes during different seasons. The mean annual precipitation is 440 mm and the annual mean solar radiation is 5900 MJ m^{-2}. The natural vegetation type is grassland. The intermixed fluvial and aeolian landforms are subject to periodic intensive rainfall and winds that cause the severe soil erosion (Fan et al., 2010). To reduce wind speeds and to prevent the drifting of sand as well as to improve the fragile ecosystem, vegetation restoration projects were performed that abandoned annual crop cultivation in favor of establishing more permanent vegetation. This involved planting trees, orchards, or/and pastures has been ongoing during the past 40 yr. The *S. matsudana* trees in the study area were planted in the aeolian sandy soil 30 yr ago. However, the growth of the trees during this time has been poor resulting in sparse canopies and stunted trunks. The poor growth is attributable to severe water stress that is due to the limited precipitation, high evaporation rates from the soil surface, and the poor water retaining capacity of the coarse textured soil with its large pore sizes (Peng et al., 2015). The sand, silt, and clay contents of the soil were 92, 7, and <1%, respectively. The soil bulk density was 1.55 g cm^{-3}.

Data were obtained from the small stand of 10 *S. matsudana* trees, which had diameters at breast height (DBH) ranging from 12.0 to 14.6 cm and were spatially distributed relatively evenly. The level of homogeneity within the stand was relatively high due to a number of factors. The stand was growing on a smooth 5° slope with a northeast aspect. The sandy soil was formed as a result of long-term aeolian deposition. Consequently, the aeolian sandy soil properties had naturally induced low degrees of variability and the soil was relatively homogenous in the layer immediately below the soil surface. Land cover was similar and there were no physical landscape features adjacent to the stand. Thus, the stand was not over shadowed by anything that would have affected solar inputs and, hence, these factors increased ET homogeneity. The area of the stand enclosed by an outer boundary, which was defined by the outer edges of the stand's tree canopies, was about 56 m^2. We selected three sample trees, described in Table 1, within the stand for sap flow determinations, while evaporation was determined from the bare soil in the center of the area enclosed by the three sample tree trunks.

Instruments: Description and Installation

The design of the three-needle HPP that we used was identical to those used and described by Ren et al. (2003), Heitman et al. (2008a, 2008b), and Xiao et al. (2011). Each HPP consisted of three parallel stainless steel needles with a diameter of 1.3 mm, a length of 40 mm, and an equidistant needle-to-needle spacing of 6 mm. Each needle contained a thermistor by which the temperature at a point, 15 mm from the tip of the needle, could be measured. In addition, the central needle contained a resistance heating wire, through which a small current of short duration could be applied to generate a heat pulse of known magnitude that could be determined by applying Joule's laws.

Table 1. Relevant parameters of the three sample *Salix matsudana* trees.

Parameter	Tree 1	Tree 2	Tree 3
DBH†, cm	13.4	13.1	14.6
Sapwood depth, cm	1.43	1.39	1.55
Sapwood area, cm^2	46.7	43.9	57.7
Plant height, m	4.1	4.4	4.6
Canopy size, m, in diameter	2.3	2.1	3.9

† DBH, diameter at breast height, taken as 1.3 m above the soil surface.

The heat-pulse measurements were performed during day of year (DOY) 230 to 294 in 2014. One HPP was inserted into the sapwood of each of the three sample trees at a height of 1.3 m above the soil surface. Before installation, coarse bark was removed at the probe insertion position, and an electric drill (bit size: 1.2-mm diam.) was used to drill three vertically aligned holes in the axial direction at a spacing of 6 mm (Fig. 1a). The probe needles were then inserted into the holes taking care to position the needles so that the temperature sensing locations were in the middle part of the sapwood; information about the distribution of the sapwood had been previously determined by coring using a tree growth cone. The exposed parts of the needles were wrapped with thermal insulation tape to prevent the upper- and lower-needles from being heated by heat transference through air. The exposed parts of the entire HPP arrangement were completely wrapped with thermal insulation tape to protect it from rain, wind, and sudden ambient temperature drifts, etc.

Five HPP were also installed at five different depths just below the surface of an area of bare soil that was surrounded by the three sample trees (Fig. 1b). Before installation, the precise needle-to-needle spacing of HPP was determined from heat pulse

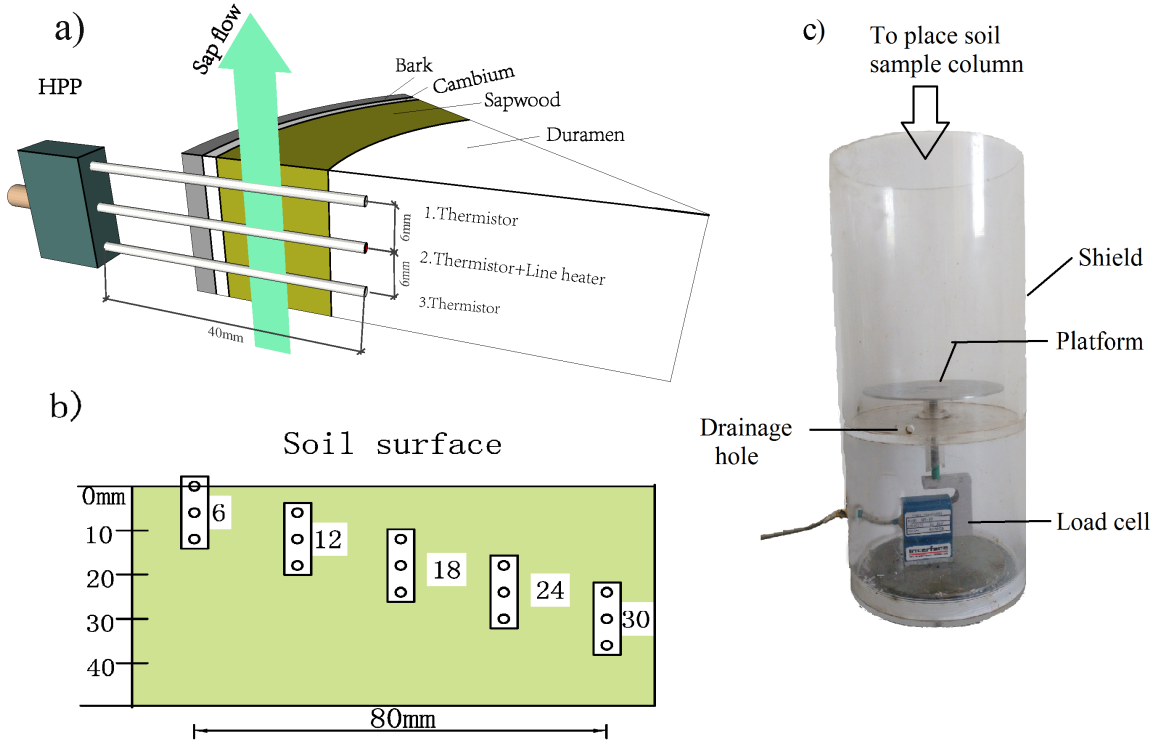

Fig. 1. (a) Schematic diagram of a three-needle heat-pulse probe (HPP) insertion in a tree trunk to determine sap flow; (b) five HPP-sets arrangement used to determine evaporation (E) in subsurface soil layers; and (c) annotated photograph of part of an automatic weighing microlysimeter (MLS).

measurements made in agar-stabilized water (Ren et al., 2003). A narrow shallow trench was dug, and the probes were inserted horizontally, with the three needles in vertical alignment. The five different HPP arrangements positioned at the five different depths were also positioned with a horizontal displacement of 20 mm to eliminate interactions with neighboring probes. The central needles of the five HPPs were positioned at depths of 6, 12, 18, 24, and 30 mm. Subsurface evaporation could thus be obtained for the separate layers at 3 to 9, 9 to 15, 15 to 21, 21 to 27, and 27 to 33 mm, which provided an evaporation profile for the entire 3- to 33-mm layer. The trench was then carefully backfilled with soil. Details of the heat-pulse operations and measurements are given below. Calculations of E and v_s from the data collected using HPP, up-scaling the v_s of the individual trees to obtain the stand T and, thence, to the determination of ET are described in the theoretical section below.

All of the HPP data, that is, for both sap flow and subsurface evaporation determinations, were collected by a data logger CR23XTD (Campbell Scientific, Logan, UT). Heat-pulse measurement sequences were performed every 30 min. For sap flow, each measurement sequence consisted of a 20-s period for background temperature measurement, followed by the generation of a 5-s heat pulse from the heating needle, and a 155-s period for temperature measurements after heating. For evaporation, the measurement sequence similarly consisted of a 20-s background temperature measurement, but this was followed by the generation of a longer 10-s heat pulse and a shorter 150-s period of temperature measurements after heating. In both cases, the total 180-s sequence of temperature responses with time of the three needles was recorded in 1-s intervals. The 20-s background temperature measurement was used to remove ambient temperature drift from the subsequent observed temperature changes over time. Sap flux density was determined every 30 min and was then averaged hourly to be synchronized with the time steps used to determine E. To determine evaporation, the soil thermal diffusivity (α, $m^2\ s^{-1}$), volumetric heat capacity (C, $J\ m^{-3}\ °C^{-1}$), and thermal conductivity (λ, $W\ m^{-1}\ °C^{-1}$) were determined every 30 min, and the E value was obtained for each hour.

Three TDP gauges were also installed on the sample trees to make additional sap flow measurements for reference purposes. This method is one of most commonly used sap flow approaches owing to its simplicity, high degree of accuracy and reliability, and relatively low cost (Lu et al., 2004). Bush et al. (2010) conducted a calibration of TDP on two common types of stem species, that is, diffuse-porous trees and ring-porous trees, and selected a range of tree species within each type. Results showed that the calibrations parameter of the ring-porous trees species were all very close to the original calibration parameters recommended by Granier (1987). The species of trees in our study, *Salix matsudana*, is classified as a typical ring-porous species. A TDP gauge consisted of a pair of stainless-steel needles (1.3 mm diameter; 13 mm long) inside which were thermocouples to sense temperature. One of these needles also acted as a heating needle and contained a resistance wire that acted as the heat source. A TDP gauge was installed in the sapwood of each sample tree, 10 cm above the HPP installation position. The heating needle with a thermocouple was vertically aligned 4 cm above the needle that only had a thermocouple; thus, the two needles measured the temperature changes in the flowing sap. The heating needle was heated by passing a small constant direct current through the resistance wire. Sap flux density was then determined from the recorded data of the temperature difference between the two needles following the procedure of Granier (1987). Further details of the TDP construction and methods of measurement are given in our previous study by Peng et al. (2015). The TDP were all connected to a CR1000 data logger (Campbell Scientific, Logan, UT) and sap flow data were collected every 30 min.

Five automated weighing MLS were used to calculate the daily E from the collected mass loss data. The MLS were made from a polyvinyl chloride column (15 cm long; 10.5 mm inner diameter; wall thickness 3 mm) that was supported by a platform connected to a load cell (SM-10, Interface MFG., Scottsdale, AZ) by a hollow steel rod. The load cell was fixed in the bottom center of a methyl-methacrylate cylinder that acted as a shelter with an open top. The top rim of the shelter was level with the top rim of the MLS when the latter was placed inside of it. The shelter was kept vertically embedded into the soil, with the top rim about 1 cm higher than the soil surface. An annotated photograph of the automated weighing MLS is shown in Fig. 1c.

Undisturbed soil samples were collected with the columns within the study stand area. The column was tapped into the soil with a rubber hammer until the top rim was level with the soil surface. The column with its intact soil sample was then carefully removed from the soil and the base sealed with gummed tape, and they were then placed on a load cell platform within an embedded shelter cylinder. The MLS were inserted into the soil adjacent to that surrounding the buried HPP-sets. The soil samples in the MLS were replaced regularly, that is, either when a rainfall event had occurred or 7 d had passed. This was done to avoid large discrepancies between the soil water conditions and soil properties in the MLS and those in the surrounding soil. These discrepancies would result in differences in the evaporation processes that occurred within and outside of the MLS, which would have increased E determination errors.

Two EC-5 moisture sensors (Decagon Devices, Pullman, MA) were inserted at soil depths of 25 and 45 mm to monitor subsurface soil volumetric water content (VWC, $cm^3\ cm^{-3}$). All of the MLS and EC-5 sensors were connected to a data logger CR10XTD (Campbell Scientific, Logan, UT). Data were collected at 10-min intervals. The VWC of the 0- to 600-cm soil profile was obtained by using a neutron probe (CNC503B (DR),Super Energy Nuclear Technology Ltd., Beijing, China) at three locations (replicates) within the study stand. Soil profile VWC was measured at 10-cm intervals in the upper 100-cm soil depth, and at 20-cm intervals in the deeper 100- to 600-cm depth, and observations were performed once a month during the study period. At the same three locations, a rainfall collec-

tor enabled the rainfall amount to be measured. These data were used to obtain ET using the water budget method.

Basic Theory of the Heat-Pulse Method

Estimations of soil water evaporation made using HPP are based on sensible heat balance theory (Heitman et al., 2008a, 2008b). The latent heat, the energy required to transform water from the liquid to vapor phase, can be derived from sensible heat balance terms, that is, the sensible heat inputs, the sensible heat outputs, and the change in sensible heat storage for a given soil layer:

$$LE=(H_u-H_l)-\Delta S \quad [1]$$

where L (J m^{-3}) is the volumetric latent heat of vaporization; E (m s^{-1}) is the evaporation rate; H_u (W m^{-1}), and H_l (W m^{-1}) are the soil sensible heat fluxes at the upper and lower boundaries, respectively, of a specified soil layer; and ΔS is the change in sensible heat storage (W m^{-1}) of the soil layer. The values of H_u and H_l were calculated as the product of the temperature gradient and the soil thermal conductivity (λ, W m^{-1}°C^{-1}). The value of ΔS was calculated as the product of the measured soil volumetric heat capacity (C, J m^{-3} °C^{-1}) and the change in temperature with time from the sensor needles (°C s^{-1}), and the depth increment (m). The latent heat was a function of time for a given soil depth layer. Sakai et al. (2011) found that using the local value of λ between each heater needle and temperature sensor needle, instead of averaging λ in both directions from the heater needle, would significantly improve the accuracy of both laboratory- and field-based E estimates. Therefore, we used the local thermal properties to determine the sensible heat terms. Total subsurface evaporation was obtained by integrating the values of individual soil water evaporation obtained from the HPP-sets installed at different depths.

Sap flow determination made using HPP was mainly based on the HRM developed by Burgess et al. (2001). This method follows the heat conduction-convection theory put forward by Marshall (1958) for conductive materials. In addition, by incorporating improvements to the compensation heat pulse method, HRM was capable of measuring low and even reverse rates of sap flow. The method used the ratio of the temperature increases detected by the upper and lower needles that were located at the same distance from a central heated needle. It considered the measurement time, probe misalignment, wound size, and sapwood thermal diffusivity. The raw heat pulse velocity (V_h, cm h^{-1}) was calculated by:

$$V_h=\frac{4\kappa t\ln(\Delta T_u/\Delta T_l)+(x_u^2-x_l^2)}{2t(x_u+x_l)}3600 \quad [2]$$

where x_u and x_l are the respective corrected needle spacings (cm) of the upper and lower needles to the central heating needle, and the correction takes into account probe misalignment and thermal diffusivity differences in the direction and counter-direction of the sap flow (for details see: Burgess et al. (2001)); $\Delta T_u/\Delta T_l$ is ratio of temperature increases detected by the upper and lower needles after time (t, s), following the emitted heat pulse; and κ denotes the thermal diffusivity (cm^2 s^{-1}) of greenwood in the axial direction. The value of κ was determined simultaneously using the T-max methods proposed by Cohen et al. (1981) that use the time (t_M, s) for the upper needle to attain the maximum temperature increase following the heat pulse emission under zero flow conditions, which are taken to exist when $\Delta T_u/\Delta T_l$ is minimal under the same conditions.

$$\kappa=\frac{x_u^2}{4t_M} \quad [3]$$

The corrected heat pulse velocity (V_c, cm h^{-1}) was obtained by multiplying V_h by a factor of B:

$$V_C=B\ V_h \quad [4]$$

where the value of B was related to the specific wound size caused by the probe insertion and any heating injury (Burgess et al., 2001).

Sap flux density (v_s, cm^3 cm^{-2} h^{-1}) was determined on an areal basis by measuring the ratio of sap to wood in the xylem and accounted for their different densities and specific heat capacities, such that v_s was related to V_c as:

$$v_s=\frac{V_c\rho_b(c_w+m_c c_s)}{\rho_s c_s} \quad [5]$$

where ρ_b (g cm^{-3}, dry weight/green volume) is the bulk density of wood; c_w and c_s are the specific heat capacity of the wood matrix (1200 J kg^{-1} °C^{-1} at 20°C, see: Becker and Edwards, 1999) and sap (water, 4182 J kg^{-1} °C^{-1} at 20°C, see: Burgess et al., 2001), respectively; m_c is sapwood water content; and ρ_s (g cm^{-3}) is the density of water, which approximately equals 1 g cm^{-3}. Parameters ρ_b and m_c could be determined from dried sapwood core samples, but the ρ_b determination also requires draining the sample before drying to measure the sapwood green volume. Volumetric sap flow (S, cm^3 h^{-1}) was then determined from the product of v_s and the cross-sectional area (cm^2) of the conducting sapwood.

Up-scaling the sap flow (S_i, cm^3 h^{-1}) data obtained at the tree scale, where the subscript i denotes the number of the sample tree, to stand level T (T, mm h^{-1}) is an important issue. The effective land area of the sample tree sap flow is determined by the area (A, m^2) of the whole forest stand and the fraction (f_i) of a sample tree's biometric parameter; for instance, its DBH or canopy size (Cermak et al., 2004). The estimation of T used a weighted mean of sap flows of the sample trees distributed for a specific sap flow area, given by:

$$T=\sum p_i S_i f_i^{-1} A^{-1}\times 10^{-3} \quad [6]$$

where p_i denotes the fraction of tree numbers classified in same category as the ith sample tree. Finally, ET (mm) was determined by summing the E (mm) and T (mm) values for a specific time step.

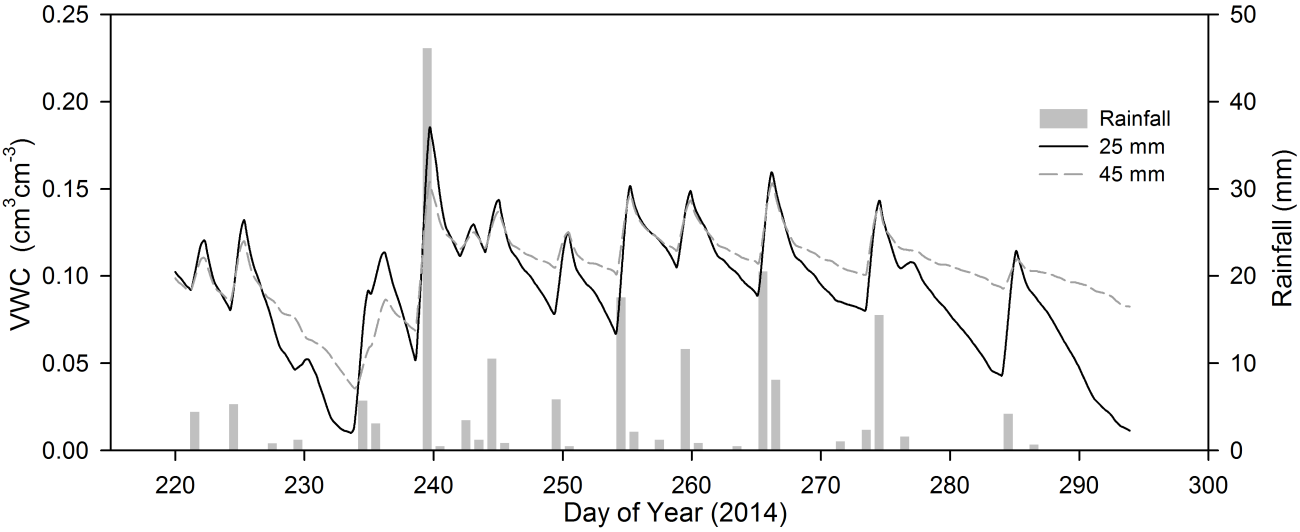

Fig. 2. Rainfall amounts and volumetric water contents (VWC) at soil depths of 25 and 45 mm during the study period (Day of Year [DOY] 230 to 294).

RESULTS AND DISCUSSION

Field Conditions

The experiments lasted 65 d, and 23 rainfall events occurred that yielded 166.7 mm, and six of these events exceeded 10 mm; the largest rainfall event (47 mm) occurred on DOY 239 (Fig. 2). The subsurface VWC at depths of 25 and 45 mm, which were measured by two EC-5 moisture sensors, are also shown in Fig. 2. The value of VWC at a depth of 25 mm ranged from 0.01 to 0.18 cm^3cm^{-3} with a mean value of 0.09 cm^3 cm^{-3} and, at a depth of 45 mm, it ranged from 0.04 to 0.15 cm^3 cm^{-3} with a mean value of 0.10 cm^3 cm^{-3}. There were distinct changes in the VWC that corresponded to the wetting and drying processes in the subsurface soil layers in response to individual rainfall events, water movement and water losses through E. The upper layer (25 mm) underwent greater changes in VWC than the deeper layer (45 mm). Generally, differences between VWC of the two layers increased with the duration of the drying process after rainfall events. In the upper layer, as the drying process continued, VWC could decrease to as low as 0.01 cm^3 cm^{-3}, that is, the layer was almost completely dried. In contrast, VWC remained above 0.08 cm^3 cm^{-3} in the lower layer in most cases.

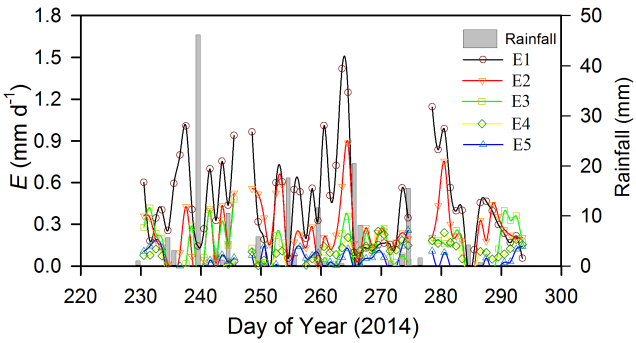

Fig. 3. Rainfall and daily evaporation rates (E) from five contiguous soil layers in the upper near surface soil layer (3–33 mm) measured by the heat-pulse probe method during the study period (Day of Year [DOY] 230 to 294).

Evaporation Measurements

Daily soil water E from a specific soil layer was obtained from of the hourly E rates calculated from the respective HPP-set of the five HPP-sets during one 24-h period. Daily E rates varied according to the depth and the date (Fig. 3). In the DOY 230 to 294 observation period, the daily E rates from the 3- to 9-, 9- to 15-, 15- to 21-, 21- to 27-, and 27- to 33-mm soil layers, had maximum values of 1.67, 0.92, 0.48, 0.26, and 0.23 mm d^{-1}, respectively, while the total E values for those layers were 33.1, 17.8, 7.4, 5.2, and 1.7 mm (Fig. 3). Depth-integrated subsurface E values for the 3- to 33-mm layer totaled 67.3 mm. Evaporation was also estimated from the data collected from the five MLS (Fig. 4). During the observation period, the mean MLS E varied between 0.04 and 3.62 mm d^{-1} and totaled 77.8 mm, which was 10.5 mm or 13.4% higher than the HPP E. The percentage contributions of the E values determined by HPP for the five individual layers to a total E value (77.8 mm) that was based on the MLS E amount were 43.5, 23.8, 9.7, 6.7, and 2.2%, respectively. This clearly demonstrated that E primarily occurred within the upper 21-mm soil layer, which accounted for more than 77% of the total MLS E.

A correlation analysis was performed to test the agreement between the values of E determined by the HPP and MLS methods (Fig. 5). The regression analysis showed that there was a highly significant ($P < 0.001$) linear relationship between the E values obtained by either using the HPP method or the MLS method, with a slope of 0.57 and an intercept of 0.31.

We also used the root-mean-square error (RMSE) and mean bias error (MBE) to test the difference between daily HPP E and MLS E; RMSE and MBE were given by:

$$\mathrm{RMSE}=\sqrt{\frac{1}{N}\sum_{i=1}^{N}d_i^2} \quad [7]$$

$$\mathrm{MBE}=\frac{1}{N}\sum_{i=1}^{N}d_i \quad [8]$$

where N is the number of data pairs, and d_i is the difference between the ith E values of the HPP method and the MLS method. During the observation period, RMSE between HPP E and MLS E was 0.54 mm d^{-1}, and MBE was -0.16 mm d^{-1} (Fig. 5).

Sap Flux Density Determination

The sapwood thermal diffusivity, κ, in the axial direction, which was obtained by the T-max method, was (2.1 ± 0.2)×10^{-3} cm^2 s^{-1} and was within the expected range of 1.4 × 10^{-3} to 4.0 × 10^{-3} cm^2 s^{-1}, which are the values for water and dry wood, respectively (Marshall, 1958). After completing all of the heat pulse measurements during the study period, the HPP sets in the sample trees were removed and wound sizes of about 2.0 mm were observed at the insertion positions of the central heating needles. Therefore, we took the wound correction coefficient, B, as 1.8905 based on the calibration table provided by Burgess et al. (2001) in relation to specific probe spacing and wound size.

The diurnal variation of v_s obtained for the three sample trees by either HPP or TDP from DOY 249 to 264 were compared with illustrate specific differences between the two methods (Fig. 6). The values of HPP v_s ranged from 0 to 12.8 cm^3 cm^{-2} h^{-1}, while those of TDP v_s ranged from 0 to 25.1 cm^3 cm^{-2} h^{-1}. The diurnal patterns of HPP v_s were similar to those of TDP v_s. However, the differences between the actual values obtained by the two methods were clearly evident. Mean HPP v_s was 3.2 cm^3 cm^{-2} h^{-1}, which was 3.0 cm^3 cm^{-2} h^{-1} or 49.3% lower than mean TDP v_s. A regression analysis was performed on the HPP v_s and TDP v_s data pairs obtained during the observation period (Fig. 7). There was a highly significant (R^2 = 0.87; P < 0.001) linear correlation between HPP v_s and TDP v_s, with a slope of 0.5235, and a zero intercept. To eliminate the systematic underestimation of HPP v_s values as compared with those of TDP v_s, we adjusted the coefficient B that was used in Eq. [4], to give B′. The value of adjusted correction coefficient, B′, was 3.611 and was obtained via a back calculation that used the regression relationship between HPP v_s and TDP v_s shown in Fig. 7. The use of B′ corrects potential errors due to wound size, tree species and applied scenarios, but it should not be used excessively without strict verification that its use gives meaningful results. The values of HPP v_s were then adjusted using B′ in Eq. [4]. These values ranged from 0.1 to 25.1 cm^3 cm^{-2} h^{-1} with a mean value of 7.45 cm^3 cm^{-2} h^{-1}. The adjusted HPP v_s was then used in further calculations.

The projected area of the small stand of 10 *S. matsudana* trees, including the 3 sample trees, was about 56 m^2. For simplicity and given that the trees were all planted in the same year and that the tree

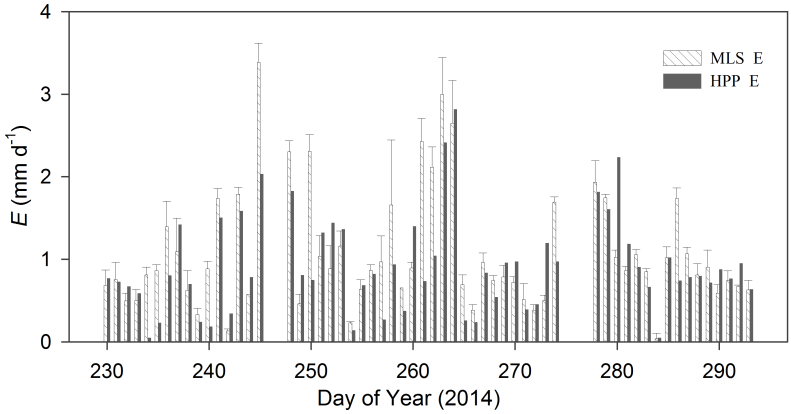

Fig. 4. Histogram of daily evaporation (E) determined by microlysimeters (MLS) and heat-pulse probes (HPP) during the study period (Day of Year [DOY] 230 to 294).

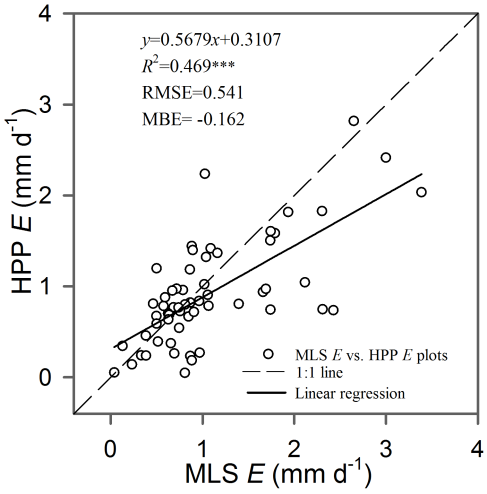

Fig. 5. A comparison of daily evaporation (E) values during the study determined either by using heat-pulse probes (HPP) or microlysimeters (MLS) using linear regression. R^2, coefficient of determination; * significant at the 0.001 probability level; RMSE, root-mean-square error; MBE, mean bias error.**

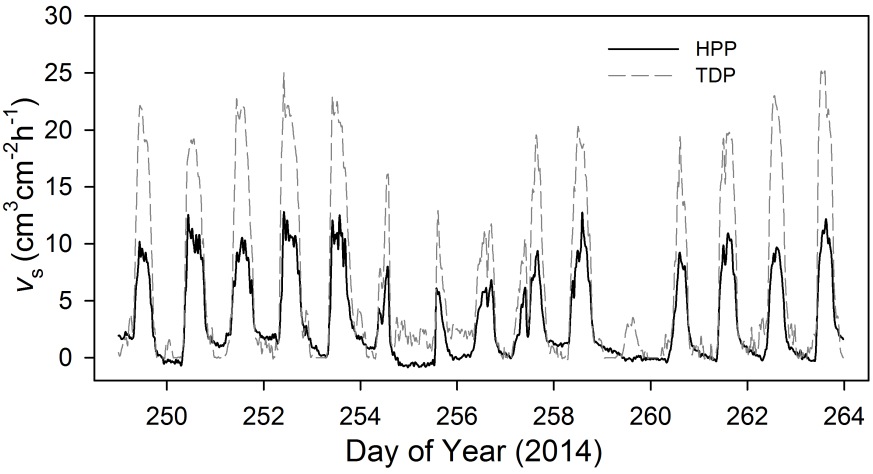

Fig. 6. Sap flux density (v_s) measured by heat-pulse probes (HPP) and thermal diffusion probes (TDP) during the study period (Day of Year [DOY] 249 to 264).

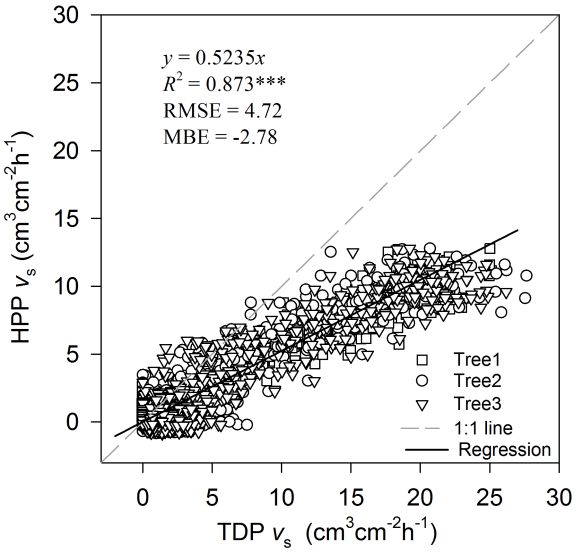

Fig. 7. A comparison of sap flux density (v_s) measured for three trees by either heat-pulse probes (HPP) or thermal diffusion probes (TDP) using linear regression. R^2, coefficient of determination; * significant at the 0.001 probability level; RMSE, root mean square error; MBE, mean bias error.**

sizes were distributed relatively uniformly, we allocated each tree an equal area of 5.6 m^2 to apportion the whole-tree sap flow during the up-scaling process. Hourly T rates, determined by HPP after up-scaling from the whole-tree level sap flow to the stand level T during the observation period are shown in Fig. 8a. Up-scaling from the whole-tree sap flow to stand level transpiration, we obtained the hourly T rates for the period from DOY 230 to 294, which are shown in Fig. 8b. The hourly T rates ranged from 0 to 0.21 mm h^{-1}, and had a mean value of 0.058 mm h^{-1}, that is, 1.39 mm d^{-1}, and exhibited great variation both within and among the days.

Evapotranspiration Determination

The hourly ET rates of the stand were calculated as the sum of E rates and T rates determined for the same 1-h time step (Fig. 8c). The maximum value of hourly ET was 0.80 mm h^{-1} and the mean value was 0.10 mm h^{-1}. Daily ET rates ranged from 0.15 to 4.8 mm d^{-1}, with a mean value of 2.4 mm d^{-1}. The total ET during the period from DOY 230 to 294 was 156.3 mm, and the corresponding E and T values were 67.3 and 89.0 mm.

We also estimated the ET value derived from the water budget by simply regarding ET as the residual of the budget terms, that is, soil water storage and precipitation, which was the only water source in the study region. Groundwater was ignored in the budget as a water source because it was too deep to have any effect on the budget. Other potential water losses could also be ignored. Runoff seldom occurred under natural conditions because of the high infiltrability of the coarse-textured sandy soil, which contained abundant macropores. Deep drainage seldom occurred because of limited deep water supplement. Furthermore, the sparse *S. matsudana* canopy meant that water losses through canopy interception could be considered negligible. Consequently, we calculated the water-budget-based ET value to be 135.3 mm during the period of DOY 230 to 294, based only on data collected from three replications in the study stand, which was relatively homogeneous, that revealed a reduction in soil water storage of 31.4 ± 23.5 mm and the measured total precipitation amount of 166.7 mm during this period. Thus, the HPP ET value was 21 mm higher than the water-budget-based ET value during our observation period.

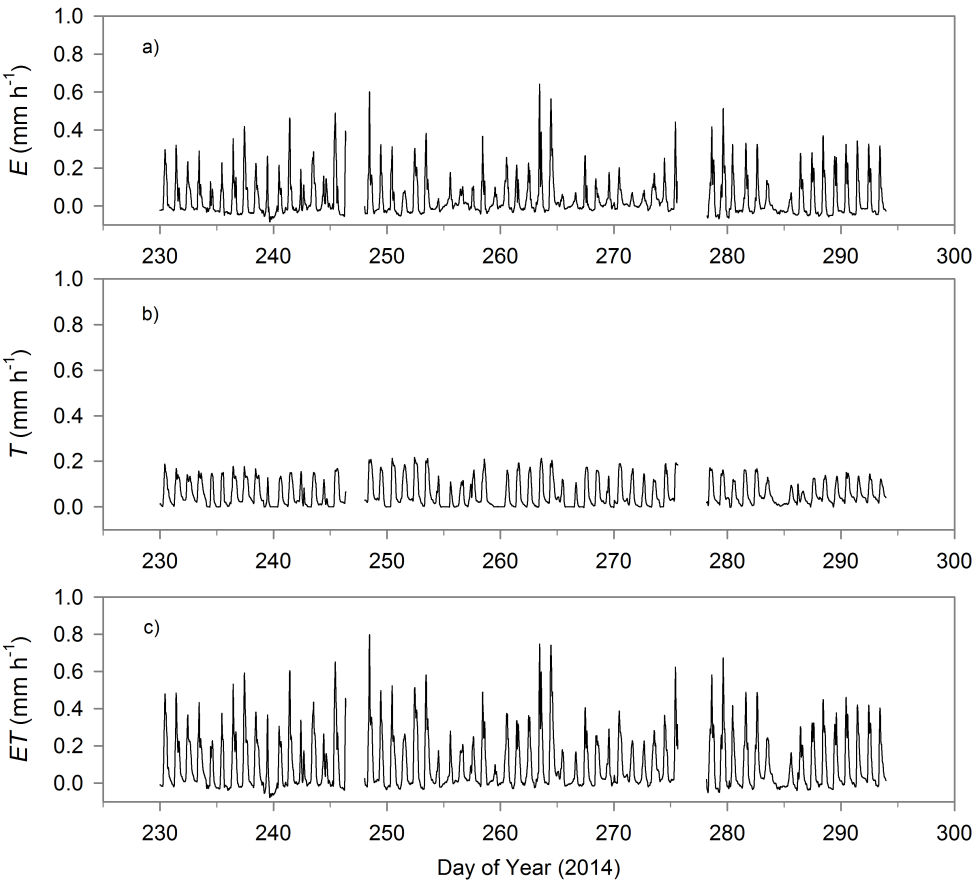

Fig. 8. Hourly evaporation (E), transpiration (T), and evapotranspiration (ET) rates of the *S. matsudana* stand during the study period (Day of Year 230 to 294); T was determined by up-scaling HPP measurements of sap flow made at the tree level.

Error Analysis

The errors involved in obtaining ET by direct determination of its individual components can derive from those resulting from the separate estimations of both E and T. These errors are now discussed briefly:

1. Errors in E measurements. The accurate determination of E when using HPP is based on making precise determinations of soil thermal properties, that is, thermal diffusivity, α, specific heat capacity, C, and thermal conductivity, λ, as well as the ambient soil temperature gradients between neighboring needles and temperature changes over a specific period. Any inaccuracies of these parameters will increase the error of the ET determination. Temperature drift caused by natural warming and cooling with the daily variation of solar radiation will distort the HPP temperature versus time curves (Jury and Bellantuoni, 1976; Zhang et al., 2014). Consequently, a noise signal is added to the temperature increments, potentially resulting in large errors in the estimation of the soil thermal properties. We eliminated the temperature drift from the observed trends in ambient temperature change over time to obtain soil thermal property values that were more reasonable by following the methods of Zhang et al. (2014). However, large errors in α and λ estimations for the data collected by the uppermost HPP-set, which was barely covered by soil, can still occur if the soil–air interface effects are not considered. Zhang et al. (2014) and Liu et al. (2013) addressed this issue using the pulsed infinite line source (PILS) theory with an adiabatic boundary condition (ABC) solution based on the work of Philip and Kluitenberg (1999). As reported by Zhang et al. (2014), using this approach to obtain accurate soil thermal properties through the built-in nonlinear model fitting functions of Mathematica software could significantly reduce the α and λ estimation errors. In this study, an attempt was made to eliminate the soil-air interface effects following their methodology. However, the fitted model could not provide reasonable parameters values. In actuality, near-surface soil heterogeneity in soil properties and soil structure affect thermal transfer, as does the temperature drift caused by frequent erratic airflow across the surface. These factors violated the underlying theoretical assumptions required for the PILS-ABC solution, and added to the complexity and uncertainty to eliminate the soil-air interface effects. We considered trying to avoid some of the problems associated with the uppermost HPP needle in the top near-surface soil layer, by using the soil thermal property values determined for the depths between the central and lower needles. This slightly deeper soil would be less exposed than the soil between the central and upper needles to the complex soil-air interface effects. Therefore, we took these values of the soil thermal properties as an approximation for those existing between the central and upper needles to calculate the various soil layer E rates and the depth-integrated total E value.

When using the approximation of the soil thermal properties, a significant albeit moderate ($R^2 = 0.47$; $P < 0.001$) linear relationship did exist between HPP E and MLS E. However, it remains challenging to estimate Stage I E (i.e., from wet soil surfaces with non-water-limited conditions) and the "undetectable zone" E from the near-surface layer between the soil surface and the midpoint between the uppermost temperature needle and the neighboring heating needle (Deol et al., 2012; Xiao et al., 2014). Even so, a modified HPP-design that reduces the probe spacing can be used to minimize the "undetectable zone". For example, an improved 11-needle HPP developed by Zhang et al. (2012) reduced the "undetectable zone" to a depth of 0.5 mm. Another approach is to supplement the modified sensible heat balance method or Bowen ratio method (Xiao et al., 2011; Xiao et al., 2014) to determine Stage I E. In our study period, the depth-integrated subsurface E value estimated by the five HPP-sets was 13.4% lower than that estimated by the MLS. The underestimation was considered to be mainly due to an inability of the HPP to detect Stage I and the "undetected zone" E. This supposition was supported by a study by Deol et al. (2014) who investigated the inception and magnitude of subsurface soil E in a wet loamy sand soil during a 5-d drying process using HPP-sets. They reported that Stage I and "undetectable zone" E terminated on the first day of drying. In the following 4 d of drying and the absence of Stage I and "undetectable zone" E, HPP-based subsurface E rates closely matched MLS E rates. The sandy soil in our study stand had a coarser texture than that of Deol et al. (2014). A greater abundance of macropores facilitated more intensive vapor diffusion and higher infiltrability, while ponding of water on the soil surface rarely occurred under natural conditions in the sandy soil. Furthermore, continuous hydraulic pathways were abundant macropores coarse textured easily broken thereby hindering the transfer of deeper soil water to the soil surface. These factors made it difficult to achieve and maintain surface wetness. Thus, Stage I E would likely have terminated even sooner than it did in the study of Deol et al. (2014) potentially reducing the error in the HPP E. However, the frequent occurrence of multiple small rainfall events in our study area would interrupt the drying process and frequently reset it to the Stage I E status, which would then increase the underestimation of HPP E.

2. Errors in T determination. Errors in T determination using HPP were primarily due to sap flow measurement errors and up-scaling errors. We applied the HRM to obtain v_s using HPP and made comparisons with estimations made by using TDP gauges. A strong and significant linear relationship existed between HPP v_s and TDP v_s, but the HPP method consistently underestimated v_s until an adjustment was made to the correction coefficient used in the HPP method. A wide range of methods can be used to measure sap flow, and these can readily identify sap flow trends but often discrepancies exist in the absolute sap flow values (Steppe et al., 2010). To our knowledge, there have been only two studies that have focused on the correction and validation of the relatively novel HRM. These were made by Burgess et al. (2001) and Bleby et al. (2004), and both only considered one tree species, Eucalyptus marginata. Errors might be related to wound diameters and sensor geometry, and to differences in tree species and sensor installation and application scenarios (Köstner et al., 1998; Fernandez et al., 2006; Steppe et al., 2010). Isarangkool Na Ayutthay et al. (2010) recommended that validation evaluations of existing correlations or re-calibrations should use gravimetric lysimeter, "cut-tree" or "cut-stems" methods as the best standards to use for comparisons, which would minimize errors.

Vandegehuchte and Steppe (2012b) emphasized that accurate estimations of sapwood thermal diffusivity, κ, is essential for sap flow determination but often it receives insufficient attention. The κ value is typically in the order of 2.5×10^{-3} cm^2 s^{-1} but accurate determinations should be made by either calculating it during zero flow conditions or from sapwood core sampling, taking into account sapwood density and water content. Although this latter method is superior to the former one, there still exist some drawbacks. 1. The water content is often taken to mean the unbound water, which ignores the bound water; this might lead to over- or underestimates of κ or v_s of 10% or more (Vandegehuchte and Steppe, 2012a). 2. Sapwood is obviously anisotropic, showing a difference in k along and across the grain, which can be up to 50% (Vandegehuchte and Steppe, 2012b). However, κ values based on sapwood density and water contents cannot estimate the correct κ value for the axial direction, which is the value that should actually be used in the conduction–convection equations for anisotropic wood to obtain v_s estimations. In our study, κ was determined by the T-max method under zero sap flow conditions, which directly determined the axial κ and thereby met the criteria for the correct application of the conduction–convection theory used in our sap flow measurements.

Up-scaling from the sample tree measured sap flow values to stand level T values was based on the DBH in our study in accordance with the suggestions of Cermak et al. (2004). The challenge is in how to determine the correct "effective" water consumption area of a tree. In our study, the stand area was relatively small and, considering the long-term water deficit conditions in the area, the trees in the stand, and especially those near the stand border, had probably extended their roots into the adjacent soil from which they could extract water, which would lead to an overestimation of T. However, this marginal effect would decrease markedly to negligible levels if the stand area was sufficiently large.

In our study, there were substantial deviations in the ET values of the three repetitions that were derived by the water budget method, with a standard deviation of 23.5 mm which was close to the change in soil water storage term (31.4 mm). This indicates that this method performs poorly especially over the relatively short 2-mo period considered in this study. In contrast, the HPP-methods potentially provide a promising means by which to determine ET at a high time-resolution as well as the data for its individual components (E and T). Furthermore, the equipment is simple and affordable. However, there remain a number of issues to be resolved to improve its performance.

CONCLUSION

This study tested the possibility of using three-needle HPP-sets to estimate ET in a small stand of *S. matsudana* stand by determining its individual components, E and T, by applying the sensible balance theory and the HRM, respectively. Results showed that, daily HPP E from the 3- to 33-mm soil layer estimated by five HPP-sets had a significant albeit moderate (R^2 = 0.47; $P < 0.001$) linear relationship with MLS E. The HPP method underestimated total E by 13.4% when compared with MLS during a 2-mo observation period. The HPP method performed well in determining v_s, which was then used to obtain stand T through an up-scaling process, when an adjustment was made to the correction factor to compensate for various sources of error; the factor suggested by Burgess et al. (2001), which corrected only for wound size led to 49% underestimations. The HPP-based ET value for the 10-tree stand was 156.3 mm between DOY 230 and 294, calculated from the sum of E (67.3 mm) and T (89.0 mm). This value was slightly higher than that obtained from the water budget method (135.3 mm).

Therefore, this HPP-based method for ET determinations in forests and orchards was considered viable. However, accuracy and applicability can be improved in a number of ways for E and T. 1. For E: Increasing the number and decreasing the spacing of HPP-sets to cover as much of the soil E zone as possible. Using HPP-sets with smaller needle spacings or modified HPP-sets, for example, the 11-needle HPP, to minimize the "undetectable zone". Supplementing experiments with the modified heat balance method or Bowen ratio method to detect Stage I E. 2. For T: Using the gravimetric lysimeter or "cut-tree" methods to determine correction factors for HPP-based sap flow measurements for specific tree species and site conditions.

ACKNOWLEDGMENTS

We acknowledge funding by The National Natural Science Foundation of China (Nos.41271239, 91025018). We are grateful to three anonymous reviewers for their helpful suggestions as well as to the editorial staff of SSSAJ.

REFERENCES

Agam, N., S.R. Evett, J.A. Tolk, W.P. Kustas, P.D. Colaizzi, J.G. Alfieri, L.G. McKee, K.S. Copeland, T.A. Howell, and J.L. Chávez. 2012. Evaporative loss from irrigated interrows in a highly advective semi-arid agricultural area. Adv. Water Resour. 50:20–30. doi:10.1016/j.advwatres.2012.07.010

Allen, R.G. 2000. Using the FAO-56 dual crop coefficient method over an irrigated region as part of an evapotranspiration intercomparison study. J. Hydrol. 229:27–41. doi:10.1016/S0022-1694(99)00194-8

Becker, P., and W.R.N. Edwards. 1999. Corrected heat capacity of wood for sap flow calculations. Tree Physiol. 19:767–768. doi:10.1093/treephys/19.11.767

Bleby, T.M., S.S.O. Burgess, and M.A. Adams. 2004. A validation, comparison and error analysis of two heat-pulse methods for measuring sap flow in *Eucalyptus marginata* saplings. Funct. Plant Biol. 31:645–658. doi:10.1071/FP04013

Bristow, K.L., G.J. Kluitenberg, and R. Horton. 1994. Measurement of soil thermal-properties with a dual-probe heat-pulse technique. Soil Sci. Soc. Am. J. 58:1288–1294. doi:10.2136/sssaj1994.03615995005800050002x

Burgess, S.S., M.A. Adams, N.C. Turner, C.R. Beverly, C.K. Ong, A.A. Khan, and T.M. Bleby. 2001. An improved heat pulse method to measure low and reverse rates of sap flow in woody plants. Tree Physiol. 21:589–598. doi:10.1093/treephys/21.9.589

Bush, S.E., K.R. Hultine, J.S. Sperry, and J.R. Ehleringer. 2010. Calibration of thermal dissipation sap flow probes for ring- and diffuse-porous trees. Tree Physiol. 30:1545–1554. doi:10.1093/treephys/tpq096

Campbell, G.S., C. Calissendorff, and J.H. Williams. 1991. Probe for measuring soil specific-heat using a heat-pulse method. Soil Sci. Soc. Am. J. 55:291–293. doi:10.2136/sssaj1991.03615995005500010052x

Cermak, J., J. Kucera, and N. Nadezhdina. 2004. Sap flow measurements with some thermodynamic methods, flow integration within trees and up-scaling from sample trees to entire forest stands. Trees-Struct. Funct. 18:529–546.

Cohen, Y., M. Fuchs, and G.C. Green. 1981. Improvement of the heat pulse method for determining sap flow in trees. Plant Cell Environ. 4:391–397. doi:10.1111/j.1365-3040.1981.tb02117.x

Deol, P., J. Heitman, A. Amoozegar, T. Ren, and R. Horton. 2012. Quantifying nonisothermal subsurface soil water evaporation. Water Resour. Res. 48:W11503 10.1029/2012wr012516.

Deol, P.K., J.L. Heitman, A. Amoozegar, T. Ren, and R. Horton. 2014. Inception and magnitude of subsurface evaporation for a bare soil with natural surface boundary conditions. Soil Sci. Soc. Am. J. 78:1544–1551. doi:10.2136/sssaj2013.12.0520

Fan, J., M.A. Shao, Q.J. Wang, S.B. Jones, K. Reichardt, X.R. Cheng, and X.L. Fu. 2010. Toward sustainable soil and water resources use in China's highly erodible semi-arid Loess Plateau. Geoderma 155:93–100. doi:10.1016/j.geoderma.2009.11.027

Fernandez, J.E., P.J. Duran, M.J. Palomo, A. Diaz-Espejo, V. Chamorro, and I.F. Giron. 2006. Calibration of sap flow estimated by the compensation heat pulse method in olive, plum and orange trees: Relationships with xylem anatomy. Tree Physiol. 26:719–728. doi:10.1093/treephys/26.6.719

Granier, A. 1987. Evaluation of transpiration in a Douglas firstands by means of sap flow measurements. Tree Physiol. 3:309–320. doi:10.1093/treephys/3.4.309

Heitman, J.L., R. Horton, T.J. Sauer, and T.M. Desutter. 2008a. Sensible heat observations reveal soil-water evaporation dynamics. J. Hydrometeorol. 9:165–171. doi:10.1175/2007JHM963.1

Heitman, J.L., X. Xiao, R. Horton, and T.J. Sauer. 2008b. Sensible heat measurements indicating depth and magnitude of subsurface soil water evaporation. Water Resour. Res. 44:W00D05 10.1029/2008wr006961.

Isarangkool Na Ayutthaya, S., F.C. Do, K. Pannengpetch, J. Junjittakarn, J.L. Maeght, A. Rocheteau, and H. Cochard. 2010. Transient thermal dissipation method of xylem sap flow measurement: Multi-species calibration and field evaluation. Tree Physiol. 30:139–148. doi:10.1093/treephys/tpp092

Jiang, B., S.L. Liang, and W.P. Yuan. 2015. Observational evidence for impacts of vegetation change on local surface climate over northern China using the Granger causality test. J. Geophys. Res. 120:1–12. doi:10.1002/2014JG002741

Jury, W., and B. Bellantuoni. 1976. A background temperature correction for thermal conductivity probes. Soil Sci. Soc. Am. J. 40:608–610. doi:10.2136/sssaj1976.03615995004000040040x

Köstner, B., A. Granier, and J. Cermák. 1998. Sapflow measurements in forest stands: Methods and uncertainties. Ann. Sci. For. 55:13–27. doi:10.1051/forest:19980102

Kool, D., N. Agam, N. Lazarovitch, J.L. Heitman, T.J. Sauer, and A. Ben-Gal. 2014. A review of approaches for evapotranspiration partitioning. Agric. For. Meteorol. 184:56–70. doi:10.1016/j.agrformet.2013.09.003

Liu, G., L. Zhao, M. Wen, X. Chang, and K. Hu. 2013. An adiabatic boundary condition solution for improved accuracy of heat-pulse measurement analysis near the soil-atmosphere interface. Soil Sci. Soc. Am. J. 77:422–426. doi:10.2136/sssaj2012.0187n

Liu, X.N., T.S. Ren, and R. Horton. 2008. Determination of soil bulk density with thermo-time domain reflectometry sensors. Soil Sci. Soc. Am. J. 72:1000–1005. doi:10.2136/sssaj2007.0332

Lu, P., L. Urban, and P. Zhao. 2004. Granier's thermal dissipation probe (TDP) method for measuring sap flow in trees: Theory and practice. Acta Bot. Sin. 46:631–646.

Marshall, D.C. 1958. Measurement of sap flow in conifers by heat transport. Plant Physiol. 33:385–396. doi:10.1104/pp.33.6.385

Ochsner, T.E., R. Horton, and T.S. Ren. 2003. Use of the dual-probe heat-pulse technique to monitor soil water content in the vadose zone. Vadose Zone J. 2:572–579. doi:10.2136/vzj2003.0572

Ochsner, T.E., R. Horton, G.J. Kluitenberg, and Q.J. Wang. 2005. Evaluation of the heat pulse ratio method for measuring soil water flux. Soil Sci. Soc. Am. J. 69:757–765. doi:10.2136/sssaj2004.0278

Ochsner, T.E., T.J. Sauer, and R. Horton. 2007. Soil heat storage measurements in energy balance studies. Agron. J. 99:311–319. doi:10.2134/agronj2005.0103S

Oki, T., and S. Kanae. 2006. Global hydrological cycles and world water resources. Science 313:1068–1072. doi:10.1126/science.1128845

Or, D., P. Lehmann, E. Shahraeeni, and N. Shokri. 2013. Advances in soil evaporation physics-a review. Vadose Zone J. 12:doi:10.2136/vzj2012.0163.

Peng, X.P., J. Fan, Q.J. Wang, and D. Warrington. 2015. Discrepancy of sap flow in *Salix matsudana* grown under different soil textures in the water-wind erosion crisscross region on the Loess Plateau. Plant Soil 390:383–399. doi:10.1007/s11104-014-2333-0

Philip, J.R., and G.J. Kluitenberg. 1999. Errors of dual thermal probes due to soil heterogeneity across a plane interface. Soil Sci. Soc. Am. J. 63:1579–1585. doi:10.2136/sssaj1999.6361579x

Qi, Y.B., Q.R. Chang, K.L. Jia, M.Y. Liu, J. Liu, and T. Chen. 2011. Remote sensing-based temporal-spatial variability of desertification and driving forces in an agro-pastoral transitional zone of Northern Shaanxi Province, China. African J. Agric. Res. 6:1707–1716.

Ren, T.S., T.E. Ochsner, and R. Horton. 2003. Development of thermo-time domain reflectometry for vadose zone measurements. Vadose Zone J. 2:544–551. doi:10.2113/2.4.544

Sakai, M., S.B. Jones, and M. Tuller. 2011. Numerical evaluation of subsurface soil water evaporation derived from sensible heat balance. Water Resour. Res. 47:W02547 10.1029/2010wr009866.

Steppe, K., D.J.W. De Pauw, T.M. Doody, and R.O. Teskey. 2010. A comparison of sap flux density using thermal dissipation, heat pulse velocity and heat field deformation methods. Agric. For. Meteorol. 150:1046–1056. doi:10.1016/j.agrformet.2010.04.004

Trautz, A.C., K.M. Smits, P. Schulte, and T.H. Illangasekare. 2014. Sensible heat balance and heat-pulse method applicability to in situ soil-water evaporation. Vadose Zone J. 13: doi:10.2136/vzj2012.0215

Trenberth, K.E., J.T. Fasullo, and J. Kiehl. 2009. Earth's global energy budget. Bull. Am. Meteorol. Soc. 90:311–323. doi:10.1175/2008BAMS2634.1

van Halsema, G.E., and L. Vincent. 2012. Efficiency and productivity terms for water management: A matter of contextual relativism versus general absolutism. Agric. Water Manage. 108:9–15. doi:10.1016/j.agwat.2011.05.016

Vandegehuchte, M.W., and K. Steppe. 2012a. Improving sap flux density measurements by correctly determining thermal diffusivity, differentiating between bound and unbound water. Tree Physiol. 32:930–942. doi:10.1093/treephys/tps034

Vandegehuchte, M.W., and K. Steppe. 2012b. Use of the correct heat conduction-convection equation as basis for heat-pulse sap flow methods in anisotropic wood. J. Exp. Bot. 63:2833–2839. doi:10.1093/jxb/ers041

Vandegehuchte, M.W., and K. Steppe. 2013. Sap-flux density measurement methods: Working principles and applicability. Funct. Plant Biol. 40:213–223. doi:10.1071/FP12233

Xiao, X.H., J.L. Heitman, T.J. Sauer, T.S. Ren, and R. Horton. 2014. Sensible heat balance measurements of soil water evaporation beneath a maize canopy. Soil Sci. Soc. Am. J. 78:361–368. doi:10.2136/sssaj2013.08.0371

Xiao, X.H., R. Horton, T.J. Sauer, J.L. Heitman, and T.S. Ren. 2011. Cumulative soil water evaporation as a function of depth and time. Vadose Zone J. 10:1016–1022. doi:10.2136/vzj2010.0070

Yu, M., and O.J. Sun. 2013. Effects of forest patch type and site on herb-layer vegetation in a temperate forest ecosystem. For. Ecol. Manage. 300:14–20. doi:10.1016/j.foreco.2012.12.039

Zhang, X., J. Heitman, R. Horton, and T.S. Ren. 2014. Measuring near-surface soil thermal properties with the heat-pulse method: Correction of ambient temperature and soil-air interface effects. Soil Sci. Soc. Am. J. 78:1575–1583. doi:10.2136/sssaj2014.01.0014

Zhang, X., S. Lu, J. Heitman, R. Horton, and T.S. Ren. 2012. Measuring subsurface soil-water evaporation with an improved heat-pulse probe. Soil Sci. Soc. Am. J. 76:876–879. doi:10.2136/sssaj2011.0052n

Zhao, N.N., Y. Liu, J.B. Cai, P. Paredes, R.D. Rosa, and L.S. Pereira. 2013. Dual crop coefficient modelling applied to the winter wheat-summer maize crop sequence in North China Plain: Basal crop coefficients and soil evaporation component. Agric. Water Manage. 117:93–105. doi:10.1016/j.agwat.2012.11.008